Chiral interactions in magnetic nanostructures

Author: Ricard Rodríguez i Dargallo
Dpt. Física de la Matèria Condensada, Facultat de Física, Universitat de Barcelona, Diagonal 645, 08028 Barcelona, Spain.

Advisor: Òscar Iglesias Clotas

Abstract: A Monte Carlo simulation program is developed to investigate the influence of the Dzyaloshinskii-Moriya interaction on the emergence of topologically nontrivial magnetic structures in two-dimensional systems. The simulation is designed to explore the conditions under which skyrmions, antiskyrmions and bimerons manifest in the presence of competing interactions. A low-temperature phase diagram for a FM thin film without magnetocrystalline anisotropy is determined along with the dependence of the aforementioned magnetic structures with the system parameters.

I. INTRODUCTION

The Dzyaloshinskii-Moriya interaction (DMI) is an antisymmetric exchange interaction that favors chiral spin structures, affecting not only domain walls, ground states and spin dynamics, but also being fundamental for the stabilization of topologically relevant structures, such as magnetic skyrmions. These magnetic structures, and therefore DMI, have captured immense interest over the last years for their potential use as fundamental bit units for high-density recording media, neuromorphic computing and spintronic applications [1]. Unlike domain walls, magnetic vortices or bubbles, skyrmions are topologically protected, which makes them resistant to external perturbations and they can be created and displaced by the application of magnetic fields or spin polarized currents in bi-dimensional systems while maintaining their shape and size due to their quasiparticle nature [2].

In order for a bulk material to be able to display DMI, it must have a crystalline structure with broken spatial inversion symmetry and its atoms must have a sizeable spin-orbit coupling, as this is the origin of DMI. Even though B20 materials such as MnSi, ferroelectrics and Heusler alloys are among the examples that satisfy both of these conditions, it is rare for a single phase material to satisfy them both, meaning that the micromagnetic DMI strength, often referred to as D, is typically weak in single phase bulk materials.

Therefore, the so-called interfacial DMI is usually considered instead. In this case, a ferromagnet is artificially grown on top of a material with strong spin-orbit coupling in order to obtain a thin film interface that presents a strong DMI (on a bulk material DMI is of the order of less than 1% of the Heisenberg exchange interaction, while interfacial DMI can represent up to more than 10%). To achieve this goal, the ferromagnetic layer is typically grown on top of a rare earth (heavy metal) film, for which spin-orbit coupling is higher due to intervention of 3d and 4d orbitals. It is also important to note that the micromagnetic DMI strength is inversely proportional to the thin film thickness [2].

A sufficiently strong DMI value can lead to the formation of unique magnetic structures such as topological defects and solitons such as skyrmions, antiskyrmions and merons. To study the conditions in which these topologically stable structures appear, we have developed a computational code based on the Monte Carlo (MC) method that incorporates the relevant interactions with the aim to study the different low temperature magnetic configurations that can be stabilized as a result of the presence of a chiral interaction such as DMI and to determine a phase diagram that allows to determine which range of parameters are necessary to obtain skyrmions in a two dimensional spin system recreating interfacial DMI.

II. MODEL AND SIMULATION METHOD

As mentioned in the introduction, the main objective of this work was to develop a versatile computational code to study the magnetic order in magnetic systems with chiral interactions. For this purpose, a 2D regular lattice having classical Heisenberg spins at its nodes has been considered. The code has been made public through a GitLab repository [3] where all the necessary subroutines written in Fortran and several Python utilities and scripts for data analysis and figure generation can be found.

The simulation software offers the possibility to work with either a squared or a triangular lattice of $N = N_x \times N_y$ spins, where N_x and N_y, along with the value of some physical constants and system parameters, can be set by the user via an input file that is read by the program at execution time. We have implemented four contributions to the total energy: magnetocrystalline anisotropy, exchange interaction, Dzyaloshinskii-Moriya interaction and Zeeman effect due to an external magnetic field

$$E = D_{ij}E_{DM} + JE_{ex} + KE_{ani} + H_{ext}E_{Zeeman} \ . \quad (1)$$

The D_{ij}, H_{ext}, J and K constants determine the relative relevance of each contribution to the total energy. In what follows, we will use $J = \pm 1$ and express all of them in dimensionless variables.

The exchange interaction being of short-range character, extends to the first nearest neighbours (nn) and its

associated energy can be written as

$$E_{ex} = -\sum_{<i,j>} \vec{S}_i \cdot \vec{S}_j \ . \tag{2}$$

The sign of J determines the ferromagnetic (> 0) or antiferromagnetic (< 0) character of the interaction, favouring parallel (or antiparallel) alignment of the spins.

The DMI energy contribution is expressed as

$$E_{DM} = -\sum_{<i,j>} \widehat{D}_{ij} \cdot \left(\vec{S}_i \times \vec{S}_j\right), \tag{3}$$

where $\widehat{D}_{ij}$ denotes the normalized DM vector, whose direction (as well as the sign and value of D_{ij}) is determined by the crystalline symmetries and geometry of the underlying heavy metal material film by the so-called Moriya rules [4, 5].

Magnetic anisotropy is considered as uniaxial along a general direction given by $\hat{n}$ and its energy contribution is given by

$$E_{ani} = -\sum_{i}^{N} \left(\vec{S}_i \cdot \hat{n}\right)^2 \ . \tag{4}$$

For ultrathin films, it usually tends to favour alignment of the spins along the direction normal to the film plane ($K > 0$ and $\hat{n} = \hat{z}$).

An external magnetic field will produce a torque to the spins of the lattice proportional to both its intensity and angle between its direction and the spin vector direction, favoring the alignment of the spins towards $\widehat{H}_{ext}$ direction

$$E_{Zeeman} = -\sum_{i}^{N} \vec{S}_i \cdot \widehat{H}_{ext} \ . \tag{5}$$

The developed program makes use of the well-known MC method implemented through the Metropolis algorithm with local updates for Heisenberg spins. As mentioned before, several properties of the system and the simulation process can be adjusted at runtime, such as the dimensions and geometry of the lattice (squared or triangular), boundary conditions (free or periodic), type of DMI to consider (see Fig. 2), number of MC steps, initial and final temperature, cooling method used (annealing or linear) and the trial method for spins (random, cone or Ising), as well as the value of the D_{ij}, H_{ext}, J and K constants, and the anisotropy and external field vectors.

The code is structured in a series of subroutines implementing several tasks as detailed in what follows. When executing the simulation software, first the data from the input file is read and the geometry of the lattice, boundary conditions and initial system configuration are set accordingly, along with the rest of the previously discussed variables. Then, the lattice positions and initial spin configuration are generated, and the set of nearest neighbours of every spin are computed and stored in a matrix, as they are required to compute the energy contributions (Eq. (2) and (3)). After this the exchange and DMI effective fields (see Sec. III for details) are computed for the initial configuration together with the total energy and magnetization. In the next stage, the system is left to evolve starting from a random spin configuration at a high initial temperature towards a low enough final temperature using the selected cooling protocol. At each temperature step, calculations of the averages of the energy and magnetisation are carried out using 50000 MC steps after discarding 1000 MC steps for thermalization purposes. Once the final temperature is reached, the final spin configuration and its DM effective fields are stored in an external file which can be used to generate arrow plots.

It is worth mentioning that the exchange and DMI effective fields are computed and stored in matrices for the initial configuration. When a MC trial change of the spin direction is accepted, only the elements corresponding to nearest neighbours of the changed spin are updated. This results in a considerable optimization and speed up in the calculation of the energy changes required by the MC method. Unless specified otherwise, the results shown in this work correspond to simulations of a squared lattice with periodic boundary conditions (PBC) and $N_x = N_y = 50$ dimensions, using the annealing cooling protocol and a random trial method for spin selection at every MC step. The final temperature for all the simulations is $T \approx 0.001J$ in order to study the ground state configurations.

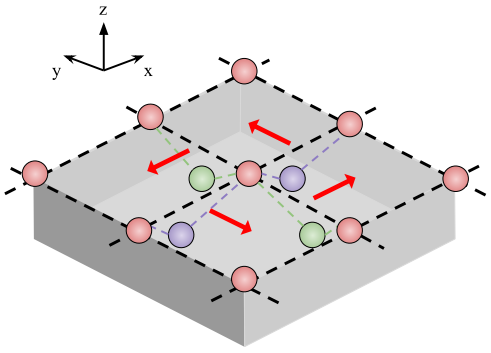

FIG. 1: Geometry and positioning of a layer of ferromagnetic atoms (red) grown on top of nonmagnetic rare earth atoms with a strong SOC (green and blue) that produces DMI vectors (red) capable of stabilizing Néel skyrmions. Figure adapted from [6].

III. DMI INTERACTION

Competition among the aforementioned interactions makes the stabilization of several spin textures possible. The DMI plays a fundamental role in the stabilization of skyrmions and other nontrivial topological structures in interfaces with broken inversion symmetry. Differently

from the typical exchange interaction term (2), this antisymmetric exchange interaction causes neighbour spin tilting, favoring the formation of chiral structures.

Skyrmions are among the topologically stable structures that can be formed due to this chiral interaction. Two different types of skyrmions can be characterized by the plane of rotation of their magnetic moments or helicity (γ) similarly to their domain walls analogs. It can be defined through the azimuthal spin component as $\Phi(\varphi) = m\varphi + \gamma$, where φ is the polar angle of the position vector and m is related to the topological charge. The spin rotation direction can either follow the radial (Néel-type skyrmion $\gamma = 0, \pi$) or azimuthal (Bloch-type skyrmion $\gamma = \pm\pi/2$) direction [7]. The sign of the DM pair constant, D_{ij}, determines the preferred direction of rotation of chiral structures (chirality). A positive value of D_{ij} will make anticlockwise rotation of spins from site i to site j more energetically favourable, while $D_{ij} < 0$ will favour clockwise rotations [8]. From now on, we will focus on the $D_{ij} > 0$ case.

Generally, in the case of interfacial DMI, the DM vectors are parallel to the lattice plane and perpendicular to the intersite radius vector connecting the two nearest neighbours ($\vec{D}_{ij} = D_{ij}(\hat{z} \times \vec{r}_{ij})$, Fig. 1), giving rise to Néel-type skyrmions [9]. Bloch-type skyrmions ($\vec{D}_{ij} = D_{ij}\vec{r}_{ij}$, Fig. 3 (b)), on the other hand, require DM vector orientations such as the ones described in the second panel of Fig. 2. However, other DM vector directions are possible depending on the system geometry (Fig. 2), resulting in the formation of different topologically nontrivial magnetic structures, as will be shown in the next section.

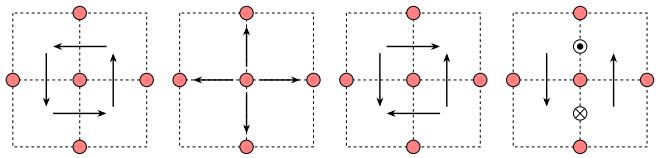

FIG. 2: From left to right, direction of DMI vectors for the formation of Néel-type skyrmions, Bloch-type skyrmions, antiskyrmions and bimerons.

It is important to emphasize that, although DMI is often claimed to be the interaction responsible for the stabilization of chiral magnetization patterns, this is not the only way to induce topologically relevant magnetic structures, nor is magnetocrystalline anisotropy necessary. It has also been shown in the literature that materials with competing or frustrated exchange interactions, or with a sufficiently strong dipolar interaction can stabilize these structures [6, 10, 11].

IV. RESULTS

Different topological states. In order to demonstrate the versatility of our code and as a benchmark to validate the implemented options, we have obtained different topologically relevant FM structures by considering different DMI scenarios displayed in Fig. 2. The configurations obtained for values of $D \simeq 1$ and $H \simeq 1$ are presented in Fig. 3, each of them corresponding to different DM vector orientations. As described in Sec. III, structures with a single value of the helicity and topological charge $Q = 1$ called skyrmions of the Neél or Bloch type are observed in Figs. 3 (a) and (b) respectively.

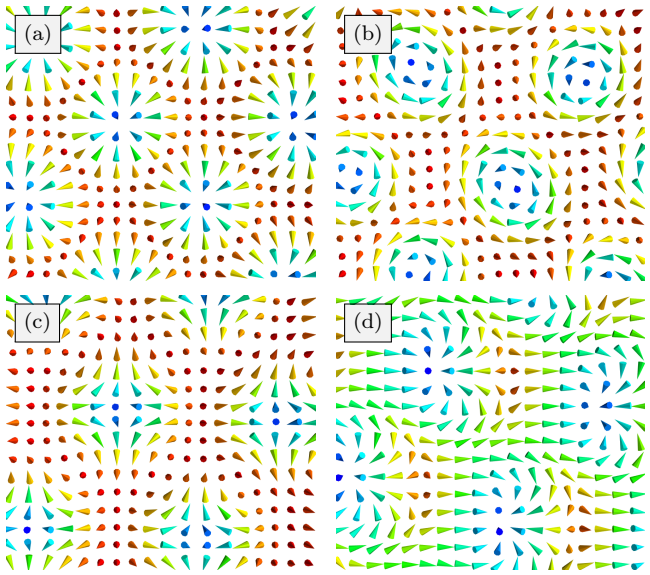

FIG. 3: Real space configurations for different topologically stable FM structures. Different colors correspond to different spin orientations along the z axis (perpendicular to the page). (a) Néel-type skyrmion. (b) Bloch-type skyrmion. (c) FM antiskyrmion. (d) Bimeron (also known as *In-plane skyrmion*).

In Fig. 3 (c) an example of the so-called antiskyrmions is shown, which are characterized by alternating Néel and Bloch type of spin rotations along the different spatial directions as dictated by the local directions of the DM vectors displayed in the third panel of Fig. 2. In all the three previous examples, topological structures appear immersed in a FM background configuration due to the application of a magnetic field perpendicular to the film plane. However, if the field is applied in the plane it is possible to stabilize a new structure made of a meron and antimeron pair with topological charges $Q = \pm 1/2$ and opposite polarities that are bound together to form a bimeron with essentially in-plane magnetization and $Q = 1$ as can be seen in Fig. 3 (d). Bimerons can also be understood as in-plane analogs of skyrmions that could be obtained by rotating the skyrmion spins around a common in-plane angle by 90° [1, 2]. In order to stabilize them, the DM vectors along one direction have to be oriented in-plane but out-of-plane along the other bond direction, as displayed in the fourth panel of Fig. 2.

Phase diagram. In this section, we focus on the case of a square lattice thin film with perpendicular DMI and no magnetic anisotropy under a magnetic field applied

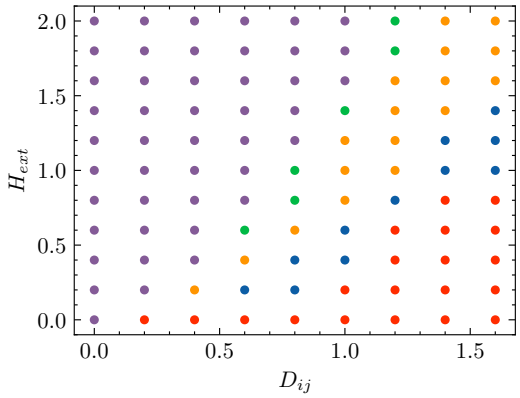

FIG. 4: Low temperature phase diagram for a FM 2D square lattice with DMI and exchange interactions under the presence of an external magnetic field. The five magnetic phases displayed are FM (purple), skyrmion gas (green), skyrmion crystal (yellow), bimerons (blue) and spiral (red).

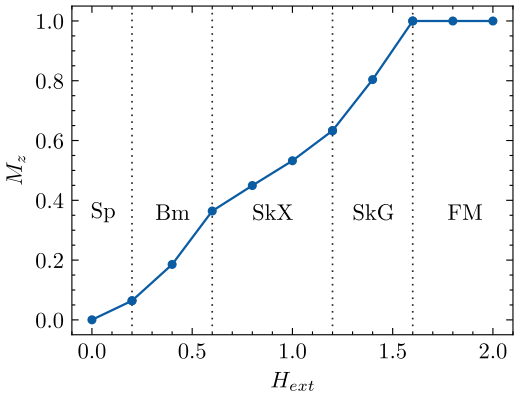

FIG. 5: Dependence of the out-of-plane magnetization component (M_z) with the external field (H_{ext}) for $D_{ij} = 1.00$.

perpendicularly to the lattice, for which we know that Néel skyrmions can be stabilized (Fig. 3 (a)). We have performed extensive MC simulations sweeping a range of values for the DMI interaction in the range $D_{ij} \in [0, 1.6]$ and a range of magnetic fields $H_{ext} \in [0, 2.0]$ for a total 99 pairs of values in order to obtain the low temperature phase diagram of the system shown in Fig. 4 and to unveil the different kinds of possible magnetic orders that can be stabilized. In order to build the phase diagram, we have inspected the magnetic configurations by direct visualization using the Mayavi Python package and classified them according to 5 different kinds of phases represented by different colors in Fig. 4. Examples of configuration snapshots taken at different regions of the phase diagram are displayed in Fig. 6.

First let us notice that if no magnetic field is applied, only spiral states similar to the snapshot (a) in Fig. 6 are obtained as a result of the competition of the exchange interaction that favours FM order (purple dots in the phase diagram) and the DMI that favours canting of the spins along the direction perpendicular to $\hat{D}$. The propagation direction of the spirals and their periodicity are determined by the kind of DMI interaction and lattice geometry. This kind of magnetic order has been observed in a variety of thin film materials but also in many bulk systems [10]. In order to obtain skyrmions, an out-of-plane magnetic field is necessary. They appear in three of the phases shown in the phase diagram, either alone or in mixed configurations: (a) skyrmion crystal, where skyrmions are arranged forming a perfect triangular lattice (yellow dots); (b) skyrmion gas (or nonperiodic skyrmion state), where skyrmions are randomly distributed across the lattice; (c) bimeron phase, in which skyrmions are mixed with elongated bimerons. The bimerons shown in Fig. 3 have a different nature than the ones appearing in the bimeron phase of the diagram. The latter ones are more akin to a rectangular shaped domain joining two skyrmions placed at the ends. Both the skyrmion gas and bimeron phases can be considered as transition or intermediate phases between the FM and skyrmion crystal phases and skyrmion crystal and spiral phases respectively [12, 13].

Skyrmion size and disposition depend on the magnetic field and the DMI. Increasing D_{ij} values result in denser skyrmion arrangements (and, therefore, smaller distance between skyrmions) that finally result in a bimeron phase, where the amount of skyrmions starts to diminish (see panels (e-h) in Fig. 6). Similarly, the periodicity of the spiral phase has a dependence on D_{ij}. Fixing a value of H_{ext} and increasing the value of D_{ij} also reduces the spiral wavelength, which is related to the D_{ij}/J ratio.

Increasing H_{ext} for a given D_{ij} gradually increases the out-of-plane magnetization. Figs. 6 and 5 show the different magnetic phases and the dependence of M_z with H_{ext} for $D_{ij} = 1.00$ in the phase diagram system. Starting from a spiral phase with no external field, magnetization increases in a significant way with the emergence of the first skyrmions in the bimeron phase. At higher H_{ext}, skyrmion density decreases, leaving a bigger amount of spins aligned in the direction of the applied field (and therefore contributing to M_z), until the FM phase is reached. As expected, in absence of DMI and/or at high H_{ext} values, the system is in a FM state.

V. CONCLUSIONS

Using a self-made simulation code including chiral interactions such as DMI competing with exchange and Zeeman terms, we have performed extensive MC simulations of a 2D square lattice thin film that have allowed us to reproduce the main topological magnetic configurations that have been evidenced in recent experiments.

We have determined a low-temperature phase diagram for a FM system without magnetocrystalline anisotropy together with the dependence of the appearance of the studied magnetic structures on the values of the material

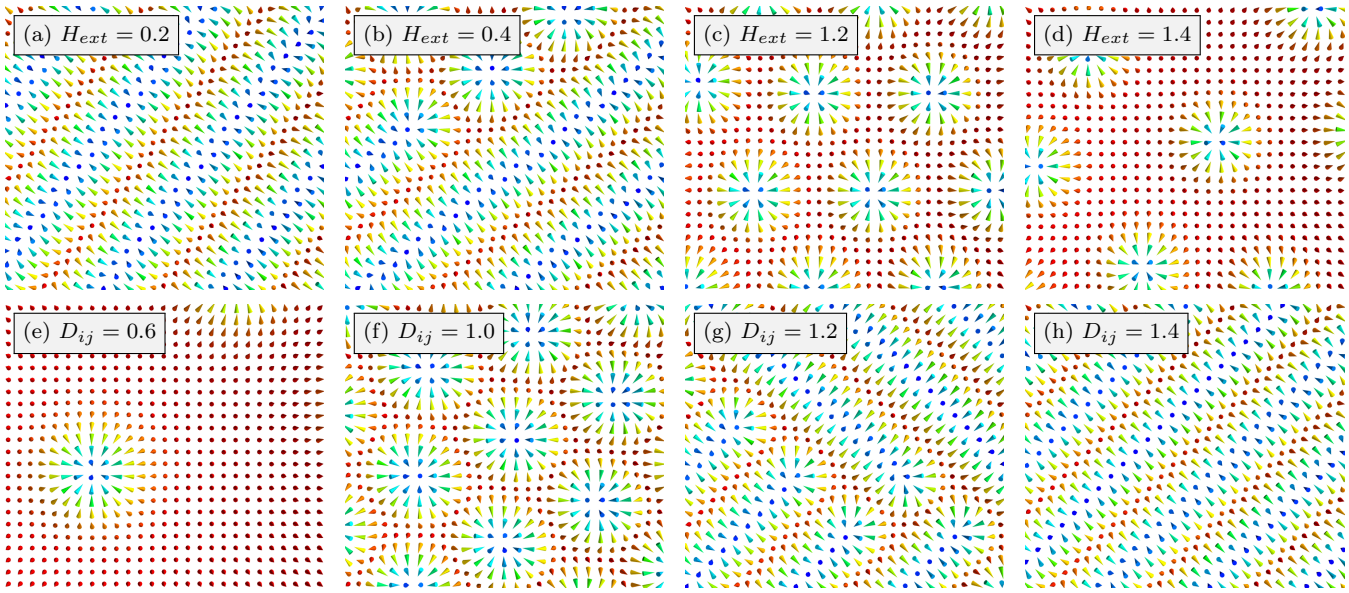

FIG. 6: Spin configurations of a FM squared lattice with no magnetic anisotropy. (a)-(d) Have a fixed value of $D_{ij} = 1.00$ and different values of H_{ext}, leading to (a) spiral, (b) bimerons, (c) skyrmion crystal and (d) skyrmion gas phases. (e-h) configurations correspond to those with a fixed $H_{ext} = 0.6$ and increasing values of D_{ij}.

dependent parameters.

In future work, the code could be extended to the study of antiferromagnets, which are promising candidates for applications, and materials having triangular lattices in which frustration could give rise to new magnetic phases. Determining the influence of in and out of plane anisotropy and observing the robustness of topological structures at finite T could also provide new and relevant information. In order to avoid errors or inaccuracies caused by the identification of magnetic phases by manual inspection of the generated 3D models, other computations and measures could also be integrated into the same code developed in this work, such as the structure factor S_q, skyrmion number, chirality or the topological charge Q, so as to be able to better characterize the studied magnetic phases. Additionally, some of the output data post-processing which was done with some external scripts could also be integrated into the main program.

Acknowledgments

I would like to thank Dr. Òscar Iglesias for his guidance and help as well as my family, friends and partner for all their support and help throughout all these years. I also acknowledge CSUC for computational resources.

[1] B. Göbel, I. Mertig, and O. A. Tretiakov, Phys. Rep. **895**, 1 (2021).
[2] R. E. Camley and K. L. Livesey, Surf. Sci. Rep. **78**, 100605 (2023).
[3] R. Rodríguez i Dargallo and O. Iglesias Clotas, "Skyrmions," (2024), Computer Software.
[4] T. Moriya, Phys. Rev. **120**, 91 (1960).
[5] A. Crépieux and C. Lacroix, J. Magn. Magn. Mater. **182**, 341 (1998).
[6] B. Göbel, A. Mook, J. Henk, I. Mertig, and O. A. Tretiakov, Phys. Rev. B **99**, 060407 (2019).
[7] K. Litzius and M. Kläui, in *Magnetic Skyrmions and Their Applications*, Woodhead Publishing Series in Electronic and Optical Materials, edited by G. Finocchio and C. Panagopoulos (Woodhead Publishing, 2021) pp. 31–54.
[8] N. Nagaosa and Y. Tokura, Nat. Nanotechnol. **8**, 899 (2013).
[9] S. Li, X. Wang, and T. Rasing, Interdisciplinary Materials **2**, 260 (2023).
[10] Y. Tokura and N. Kanazawa, Chem. Rev. **121**, 2857 (2021).
[11] Y. A. Kharkov, O. P. Sushkov, and M. Mostovoy, Phys. Rev. Lett. **119**, 207201 (2017).
[12] F. A. Gómez Albarracín and H. D. Rosales, Phys. Rev. B **105**, 214423 (2022).
[13] I. A. Iakovlev, O. M. Sotnikov, and V. V. Mazurenko, Phys. Rev. B **97**, 184415 (2018).